Current Biology 20, 2199–2206, December 21, 2010 ©2010 Elsevier Ltd All rights reserved DOI 10.1016/j.cub.2010.11.038

Report

# Acute Induction of *Eya3* by Late-Night Light Stimulation Triggers *TSH*β Expression in Photoperiodism

**Koh-hei Masumoto,[1,3] Maki Ukai-Tadenuma,[1] Takeya Kasukawa,[2] Mamoru Nagano,[3] Kenichiro D. Uno,[2] Kaori Tsujino,[1,4] Kazumasa Horikawa,[3] Yasufumi Shigeyoshi,[3,*] and Hiroki R. Ueda[1,2,4,5,*]**

[1]Laboratory for Systems Biology
[2]Functional Genomics Unit
RIKEN Center for Developmental Biology, 2-2-3 Minatojima-minamimachi, Chuo-ku, Kobe, Hyogo 650-0047, Japan
[3]Department of Anatomy and Neurobiology, Kinki University School of Medicine, 377-2 Ohno-Higashi, Osakasayama City, Osaka 589-8511, Japan
[4]Graduate School of Science, Osaka University, 1-1 Machikaneyama, Toyonaka, Osaka 560-0043, Japan
[5]Department of Mathematics, Graduate School of Science, Kitashirakawa Oiwake-cho, Sakyo-ku, Kyoto, Kyoto University, Kyoto 606-8502, Japan

## Summary

**Living organisms detect seasonal changes in day length (photoperiod) [1–3] and alter their physiological functions accordingly to fit seasonal environmental changes. *TSH*β, induced in the pars tuberalis (PT), plays a key role in the pathway that regulates vertebrate photoperiodism [4, 5]. However, the upstream inducers of *TSH*β expression remain unknown. Here we performed genome-wide expression analysis of the PT under chronic short-day and long-day conditions in melatonin-proficient CBA/N mice, in which the photoperiodic *TSH*β expression response is preserved [6]. This analysis identified "short-day" and "long-day" genes, including *TSH*β, and further predicted the acute induction of long-day genes by late-night light stimulation. We verified this by advancing and extending the light period by 8 hr, which induced *TSH*β expression within one day. In the following genome-wide expression analysis under this acute long-day condition, we searched for candidate upstream genes by looking for expression that preceded *TSH*β's, and we identified the *Eya3* gene. We demonstrated that *Eya3* and its partner *Six1* synergistically activate *TSH*β expression and that this activation is further enhanced by *Tef* and *Hlf*. These results elucidate the comprehensive transcriptional photoperiodic response in the PT, revealing the complex regulation of *TSH*β expression and unexpectedly rapid response to light changes in the mammalian photoperiodic system.**

## Results and Discussion

### Genome-wide Expression Analysis of the Mouse Pars Tuberalis under Chronic Conditions

The pars tuberalis (PT) is thought to be responsible for detecting photoperiod, by integrating circadian time and environmental light/dark information [7–9]. Recently, a genome-wide expression analysis revealed that the thyroid-stimulating hormone (TSH) pathway triggers photoperiodic responses in the Japanese quail [4, 5]. In mammals, nocturnal melatonin secretion is thought to carry environmental light/dark information to the PT [10–14], where the melatonin receptor is highly expressed [15]. However, the detailed molecular mechanism that links melatonin signals with *TSH*β expression in the PT remains unclear.

To identify the upstream inductive mechanism of *TSH*β expression, we performed genome-wide expression analyses of the PT under chronic short-day and long-day conditions in melatonin-proficient CBA/N mice, in which the photoperiodic *TSH*β expression response is preserved [6] (Experimental Procedures). The data obtained were first analyzed for circadian gene expression (see Supplemental Experimental Procedures available online) because PT contains circadian oscillators [16] (Figure S1A; Supplemental Results and Discussion). We identified 1000 significant 24 hr rhythmic genes in the PT (Figure 1A; Table S1). The identified genes included several clock and clock-controlled genes (Figure 1B; Table S2; Supplemental Results and Discussion). Their average peak time in the long-day condition was 7.71 hr later than in the short-day condition (Figure 1B), suggesting that circadian clocks in the PT are entrained to the end of a light period.

The obtained data were next analyzed to identify "photoperiodic" genes in the PT (Supplemental Experimental Procedures). This photoperiodic expression analysis significantly identified 246 "long-day" genes and 57 "short-day" genes in the PT (Figure 1C; Table S3). The identified genes included *TSH*β, which was further confirmed by quantitative PCR (qPCR) and radioisotope (RI) in situ hybridization (Figure 1D). In contrast, *TSH* α subunit (*Cga*) and *Tac1* [17] did not respond to the photoperiod in the mouse PT (Figures S1B and S1C; see details in Supplemental Results and Discussion).

### Late-Night Light Stimulation Immediately Induces *TSH*β Expression in the Mouse PT

We next examined the timescale of the *TSH*β induction after the transition from the short-day to the long-day condition. We transferred mice from the short-day to the long-day condition by delaying lights-off for 8 hr (hereafter, the "delay" condition) and sampled the PTs at zeitgeber time 16 (ZT16; ZT0 was defined as the time of lights-on) because *TSH*β is rapidly induced at around ZT16 in the PT of the Japanese quail [4]. However, in contrast to the previously reported immediate induction of *TSH*β in the quail, *TSH*β expression in the mouse PT increased gradually over the 5 days following the transition from the short- to the long-day condition (Figure 2A). Because the PT circadian clock was entrained to the lights-off timing (Figure 1B), we speculated that the observed slow dynamics of *TSH*β induction in the mouse PT were due to the gradual entrainment of the PT circadian clock. We also hypothesized that the "photoinducible" phase (the circadian time when light stimulation can induce *TSH*β expression) is in the subjective (circadian) late night (as defined in the short-day condition), and therefore entrainment over 5 days might be required for full transition of the photoinducible phase to the photoperiod under the long day.

*Correspondence: shigey@med.kindai.ac.jp (Y.S.), uedah-tky@umin.ac.jp (H.R.U.)

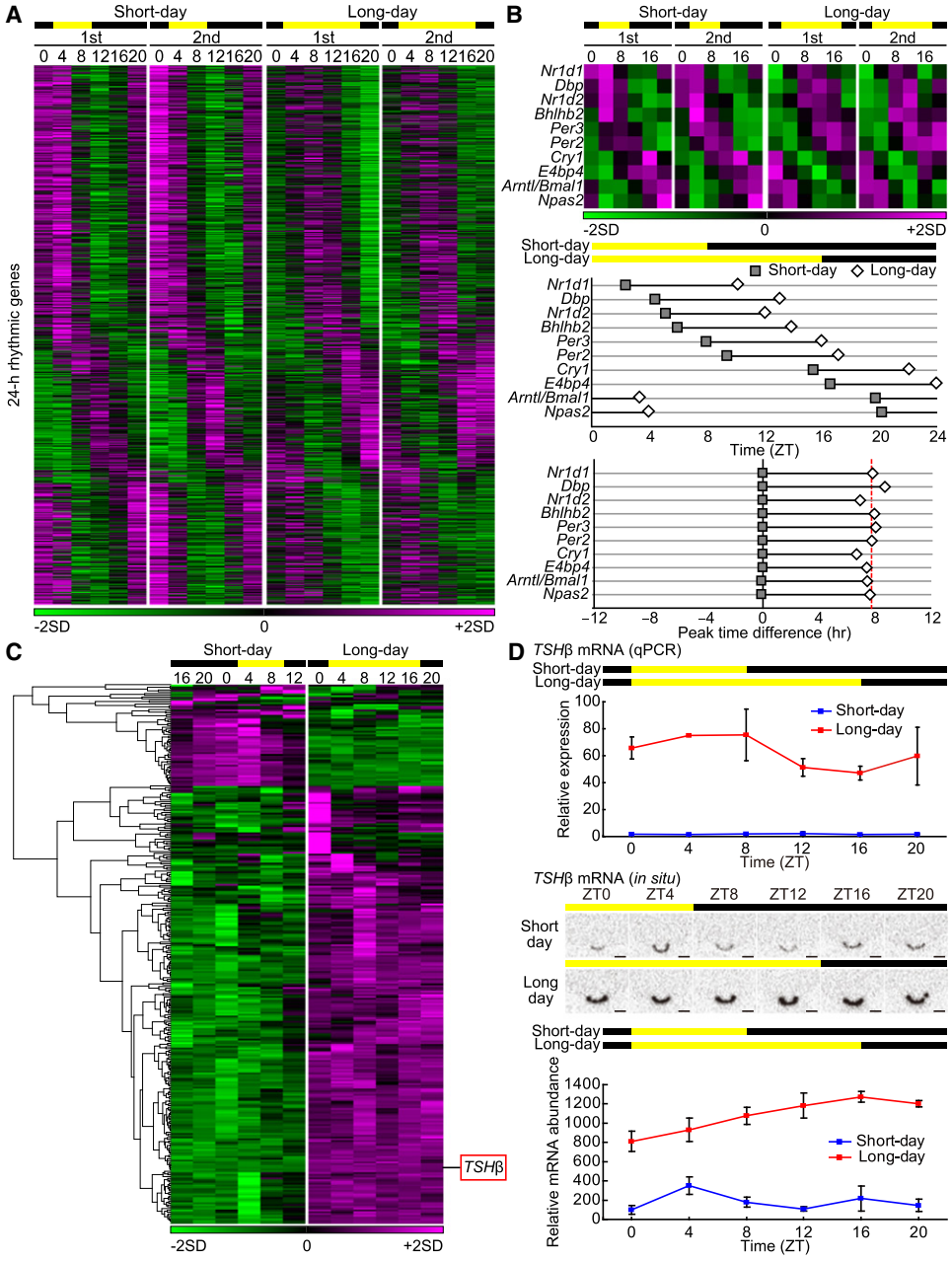


Figure 1. Genome-wide Expression Analysis of Circadian and Photoperiodic Genes in the Mouse Pars Tuberalis under Chronic Short-Day and Long-Day Conditions

(A) Heat map of 24 hr rhythmic genes in the mouse pars tuberalis (PT) under short-day (left two panels) and long-day (right two panels) conditions. In both conditions, time-series data of the first and second experimental replicates are plotted. In the heat maps in (A)–(C), magenta tiles indicate higher gene expression; green tiles indicate lower expression.

(B) Peak-time difference in the circadian expression of clock and clock-controlled genes between short-day and long-day conditions. The upper panel shows a heat map of the clock and clock-controlled genes. The middle panel shows their peak times. The lower panel indicates the difference in peak time between the short-day and long-day conditions. The peak time in the short-day condition for each gene was set to 0. The average difference in peak time was 7.71 hr (dashed red line).

(C) Heat map of photoperiodic genes for which the expression level changed between the short-day and long-day conditions. The location of *TSH*β is indicated.

(D) Confirmation of the GeneChip data for *TSH*β expression. *TSH*β expression under short-day and long-day conditions was measured by qPCR (n = 2, top panels; *TSH*β expression relative to *Tbp* expression is plotted) and radioisotope (RI) in situ hybridization (n = 3, middle and bottom panels; scale bars represent 300 μm). Error bars represent ± standard error of the mean (SEM).

To confirm that the PT circadian clock was gradually shifted in this condition, we used a molecular timetable method [18, 19], which can measure circadian phase from the expression pattern of clock and clock-controlled genes with a single-time-point sample (Supplemental Experimental Procedures). We found that the PT circadian time was

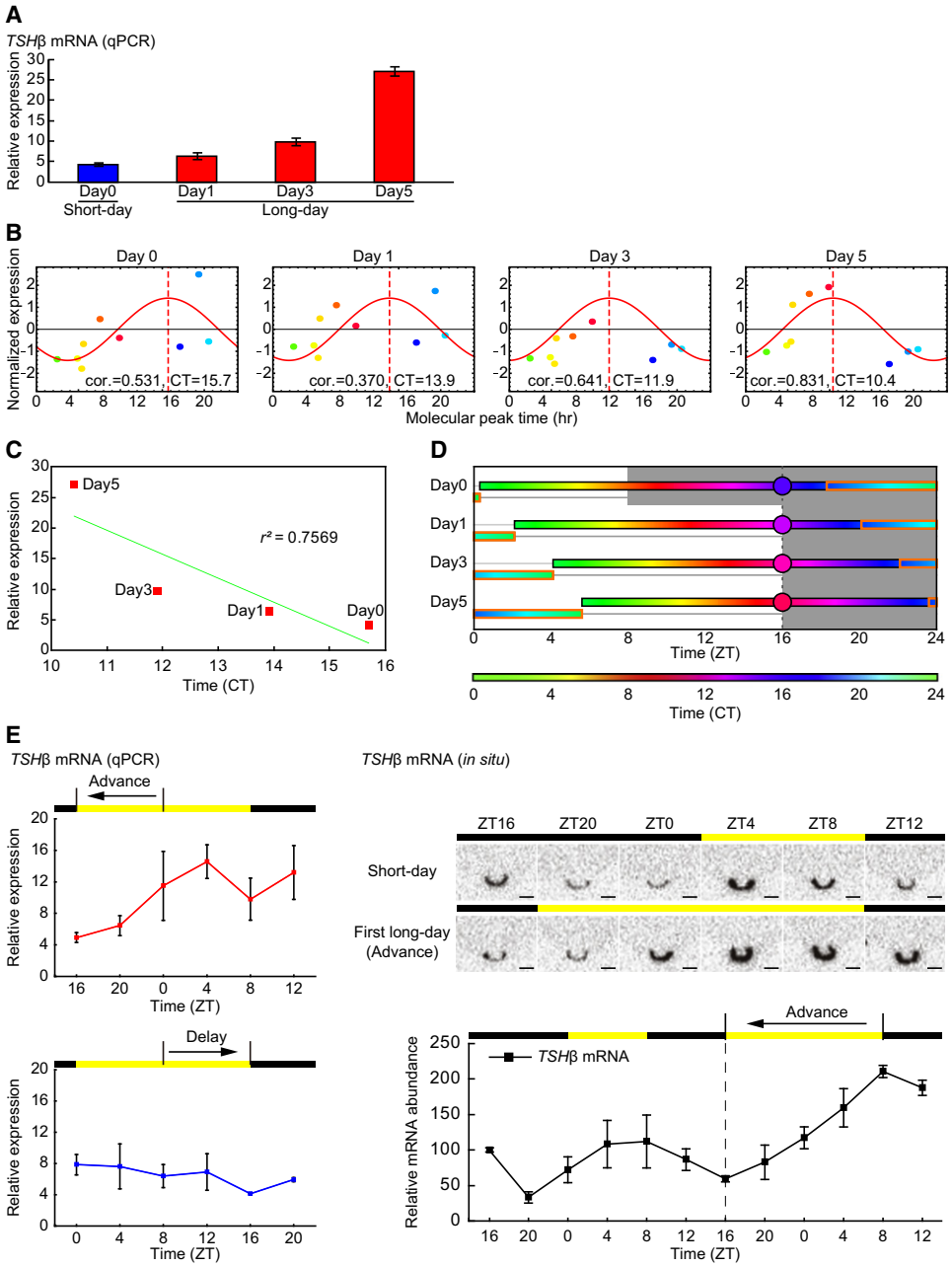


Figure 2. Late-Night Light Stimulation Immediately Induces *TSH*β Expression in the Mouse PT

(A) *TSH*β expression at ZT16 on days 0, 1, 3, and 5 after the transition of light condition, in which lights-off timing was delayed by 8 hr. *TSH*β expression was measured by qPCR (n = 2). *TSH*β expression relative to *Tbp* expression is plotted. Error bars represent ± SEM.

(B) Circadian time measurement from the mouse PT. Colors and x values of the dots indicate the molecular peak time of individual clock and clock-controlled genes. The peak time of the red cosine curve indicates the estimated circadian time (CT, dashed vertical line). The correlation coefficient (cor.) between the red cosine curve and normalized expression data is also indicated in the panel.

(C) Linear regression analysis between the estimated circadian time (CT, x axis) of the PT and quantity of *TSH*β expression (y axis). Red dots indicate data points. Green line indicates regression line. $r^2 = 0.7569$.

(D) Gradual change in the estimated circadian time of the PT from day 0 to day 5. Color bars indicate the estimated circadian time (CT) of the PT on each day. The x axis indicates the environmental zeitgeber time (ZT). The circadian time at ZT16 is indicated by a colored circle. The orange-outlined box indicates the putative photoinducible phase. The background indicates the light conditions (white, light phase; gray, dark phase).

(E) CBA/N mice kept in the short-day condition (light:dark = 8:16 hr) for 3 weeks were then transferred to a long-day condition, in which the dark period was advanced (advance condition) or delayed (delay condition) by 8 hr. Left panels: *TSH*β expression on the first long day (advance and delay conditions) was measured by qPCR (n = 2). *TSH*β expression relative to *Tbp* expression is plotted. Right panels: *TSH*β expression in the short-day condition and on the first long day (advance condition) was measured by RI in situ hybridization (n = 3). Scale bars represent 300 μm. Error bars represent ± SEM.

gradually shifted over 5 days (Figure 2B). We also noted that the circadian time in the PT correlated well with the induction of *TSH*β expression (Figure 2C; $r^2 = 0.7569$), consistent with the hypothesis. Based on these findings, we plotted the measured circadian time and the hypothesized photoinducible phase (i.e., the circadian late-night period) over the 5 days after the shift and superimposed it on the photoperiod (Figure 2D). This plot showed that *TSH*β expression was not induced on the first day as a result of the mismatch between the hypothetical photoinducible phase of the PT (Figure 2D, orange-outlined box) and the photoperiod (Figure 2D, day 1), whereas *TSH*β expression was strongly induced on the fifth day because of the match between the hypothetical photoinducible phase and the photoperiod, after gradual entrainment of the PT over 5 days (Figure 2D, day 5). This result supports our hypothesis that the photoinducible phase is in the circadian late-night period.

Furthermore, this hypothesis also predicted that *TSH*β expression would be strongly induced on the first day in an alternative long-day condition in which the lights-on timing was advanced by 8 hr (hereafter, the "advance" condition). To verify this prediction, we examined *TSH*β expression in the PT under the advance condition, and we found that it increased immediately (Figure 2E; Figure S1D). RI in situ hybridization also confirmed this immediate *TSH*β expression (Figure 2E, right panels). On the other hand, *TSH*β expression was not induced in the delay condition (Figure 2E, left-bottom panel; Figure S1D). These findings suggest that the mouse PT has a photoinducible phase during subjective late night and that light stimulation occurring in the late night can induce *TSH*β expression immediately, i.e., within one day.

### Genome-wide Expression Analysis of Acute Long-Day Genes in the Mouse PT

Given the rapid induction of *TSH*β, we reasoned that a genome-wide expression analysis in the advance and delay conditions might allow us to identify the the upstream inductive mechanism of the *TSH*β pathway. Therefore, we performed a second set of genome-wide expression analyses under these acute long-day conditions (Experimental Procedures). The data obtained were then analyzed to extract "acute long-day" genes expressed in the PT (Supplemental Experimental Procedures). This expression analysis identified 34 acute long-day genes in the PT (Figure 3A; Table S4), which included several transcription factors; *Eya3*, *Ror*β, *Maff*, *Crem*, and *Hdac4* (Figure S1D). We focused on *Eya3* as a putative upstream activator of *TSH*β expression because *Crem* and *Hdac4* encode transcriptional repressors [20, 21] and because *Ror*β and *Maff* could not activate the 7.7 kbp promoter of *TSH*β (Figures S2A and S2B). We first confirmed the acute induction of *Eya3* expression in the PT under the advance condition via qPCR and RI in situ hybridization (Figure 3B; Supplemental Results and Discussion).

### *Eya3* and *Six1* Synergistically Induce *TSH*β Expression

*Eya3* is one of four mammalian homologs (*Eya1–4*) of *eya* [22, 23], a transcriptional coactivator involved in fly eye development [24, 25]. *Eya* family members form a complex with a DNA-binding factor of the *Six* family and a corepressor of the *Dach* family. *Six-Eya-Dach* genetic interactions are reported to regulate the transcriptional activation and repression of target genes. Of the *Eya*, *Six*, and *Dach* families, we found that the *Eya3* and *Six1* mRNAs were highly expressed in the PT under the long-day condition whereas the others were weakly or barely expressed (Figure 4A). We therefore examined whether *Eya3* and *Six1* activate the *TSH*β promoter. The transient transfection of *Eya3* or *Six1* increased the *TSH*β promoter activity only slightly, whereas their cotransfection synergistically increased its activation (Figure 4B). In contrast, *Eya3* and *Six1* did not activate the SV40 promoter. We also found that shorter versions of the *TSH*β promoter (Figure 4C) were also synergistically activated by *Eya3* and *Six1* (Figure 4B). We thus used the shortest version of the *TSH*β promoter (0.1 kbp) in the following experiments unless otherwise indicated. We also confirmed that *Eya3* increased *TSH*β promoter activity in a dose-dependent manner when it was expressed alone or with *Six1* (Figure 4D; Figure S2C; Supplemental Results and Discussion).

### An So Site Is Important for *Eya3-Six1*-Dependent Activation of the *TSH*β Promoter

It has been reported that *Six* and *Eya* can activate their target genes through different consensus sequences for *Six* binding (MEF3 site, see [26, 27]; So site, see [27–29]). Therefore, we searched for Six consensus sequences in the 0.1 kbp *TSH*β promoter and found one MEF3 site (+1) and two So sites (−45 and −52) upstream of the transcription start site (TSS). These MEF3 and So sites in the *TSH*β promoter are highly conserved among vertebrates (Figure 4C). We first deleted and mutated the one MEF3 site in the *TSH*β promoter and found that it was dispensable for the *Eya3-Six*-dependent activation of the *TSH*β promoter (Figure 4E). We then sequentially deleted the two So sites (Figure 4C, So1 and So2). Although deletion of the So2 site did not affect the *Eya3-Six*-dependent activation of the *TSH*β promoter, deletion of the So1 site significantly decreased the change elicited by the *Eya3-Six*-dependent activation (Figure 4F). These results indicate that the So1 site is essential for the full activation of the *TSH*β promoter by the *Eya3-Six1* complex.

Because *Tef* can increase *TSH*β promoter activity [30], we also examined the contribution of *Tef* and its family member *Hlf* to the 0.1 kbp *TSH*β promoter. We found that *Tef* or *Hlf* synergistically increased the luciferase activity of the *TSH*β promoter when cotransfected with *Eya3* and *Six1* (Figures S2D–S2J; see details in Supplemental Results and Discussion).

### Photoinducible Phase at Subjective Late Night

In this study, genome-wide expression analyses of the mouse PT revealed that *TSH*β and *Eya3* expression are induced by late-night light stimulation. Because these expression data might include potentially important factors besides *Eya3* and *TSH*β, we have made them publicly available (http://photoperiodism.brainstars.org/). We further demonstrated that *Eya3* and its partner *Six1* are expressed in the mouse PT and synergistically activate *TSH*β expression through an So site in the *TSH*β promoter. This activation is further enhanced by *Tef* and *Hlf* through a D box close to the So site. Because previous reports described *Eya3* induction in the PT under long-day conditions in birds [4, 5] and sheep [17], its induction under long-day conditions appears to be an evolutionarily conserved molecular mechanism in the photoperiodism of vertebrates. Among the remaining challenges is the in vivo functional analysis of *Eya3*-dependent induction of *TSH*β expression.

Based on these and previous findings, we propose the following hypothetical model for a gradual transition over months from short-day to long-day conditions in the natural environment. As the photoperiod is gradually extended to

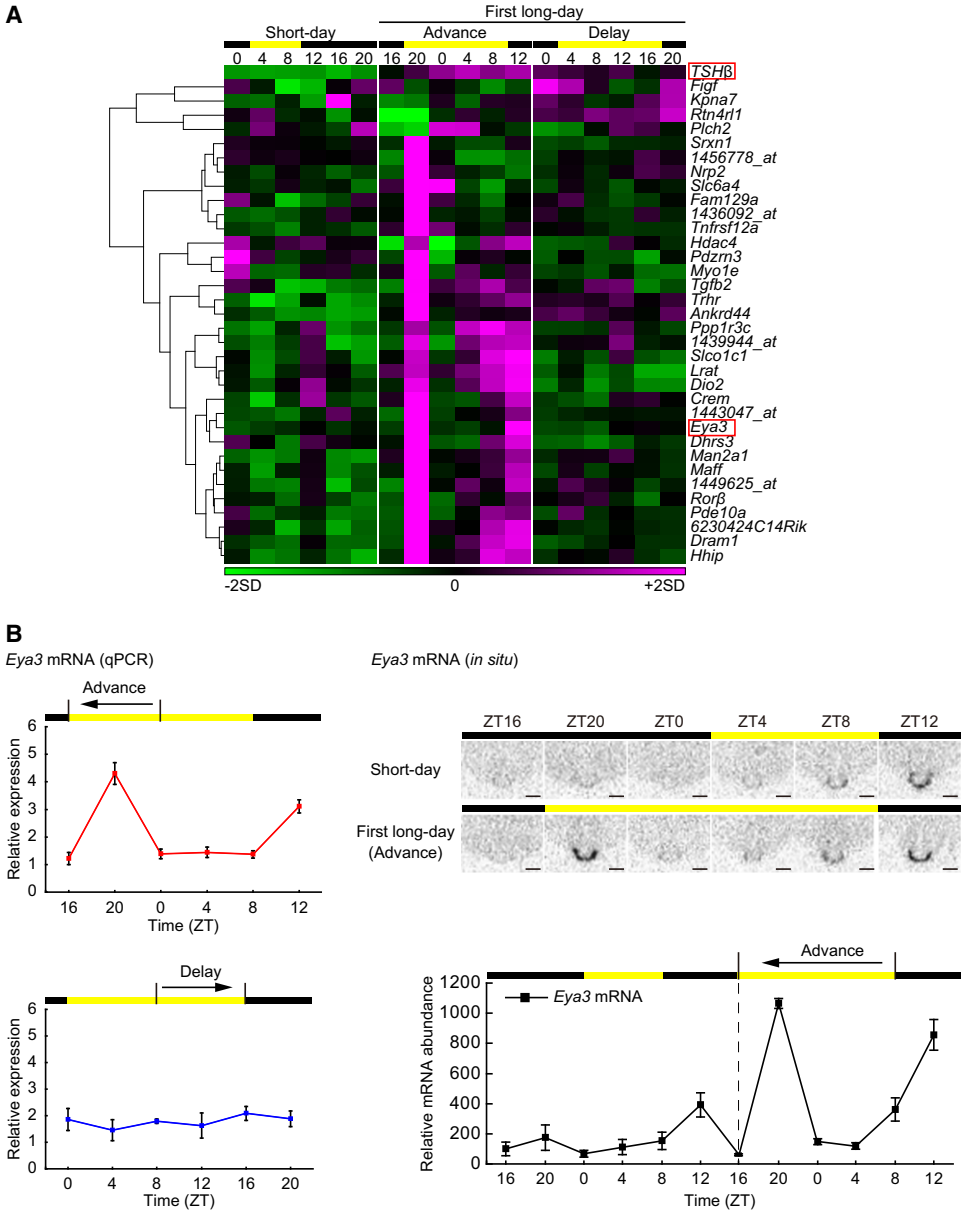


Figure 3. Genome-wide Expression Analysis of Acute Long-Day Genes in the Mouse PT

(A) Heat map of photoperiodic genes whose expression was altered by the photoperiod change only in the advance condition. Magenta tiles indicate higher gene expression in the PT; green tiles indicate lower expression. GeneChip data for *TSH*β expression are displayed for reference.

(B) Confirmation of the GeneChip data for *Eya3* expression. Left panels: *Eya3* expression on the first long day (advance and delay conditions) was measured by qPCR (n = 2). *Eya3* expression relative to *Tbp* expression is plotted. Right panels: *Eya3* expression under the short-day condition and on the first long day (advance condition) was measured by RI in situ hybridization (n = 3). Scale bar represents 300 μm. Error bars represent ± SEM.

completely cover the photoinducible phase (the subjective late night, determined in the short-day condition), *Eya3* is gradually induced, which triggers *TSH*β expression in the PT under natural conditions. These natural and relatively slow expression dynamics can be speeded up by artificial light stimulation at subjective late night, which acutely induces *Eya3* expression. This artificial situation reveals that the mammalian photoperiodic system has unexpectedly rapid dynamics and indicates that the PT of CBA/N mice is an ideal model system for elucidating the remaining molecular mechanisms of photoperiodism (Supplemental Results and Discussion). Identifying the upstream inducer of the acute *Eya3* elevation as well as elucidating the signal transduction cascade from the melatonin receptor to *Eya3* expression will provide further insights into photoperiodism.

## Experimental Procedures

### Animals and Housing

Male CBA/N mice (Japan SLC, Shizuoka, Japan), which have normal retinas (Supplemental Results and Discussion), were purchased 3 weeks after birth. For chronic long-day and short-day experiments, mice were first housed under short-day conditions (light:dark = 8:16 hr, ZT0 = lights-on, ZT8 = lights-off, 400 lux), given food and water ad libitum, and maintained under these short-day conditions for 3 weeks. The mice were then separated

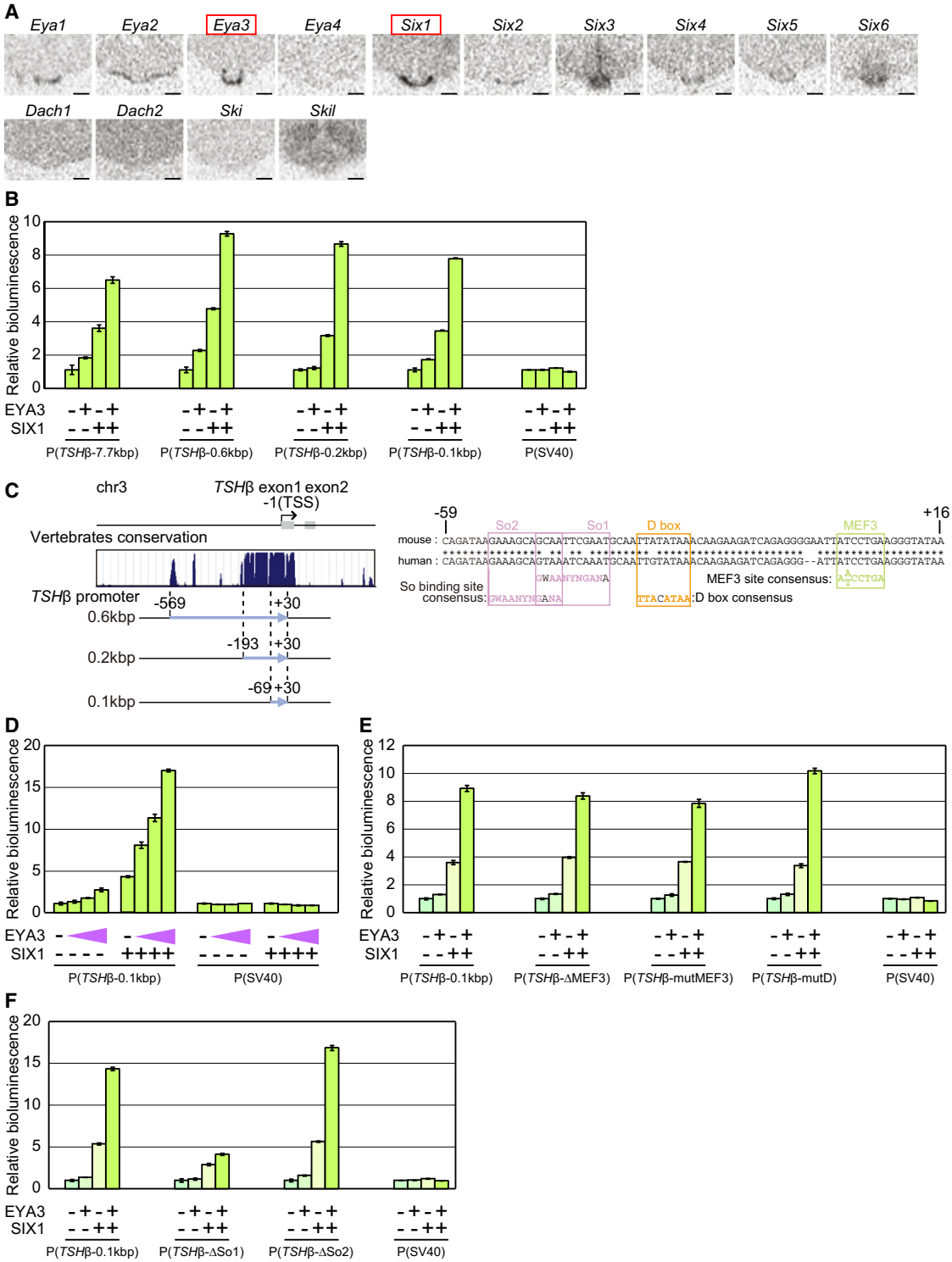


Figure 4. *Eya3* and *Six1* Synergistically Induce *TSH*β Expression

(A) Expression of the *Eya*, *Six*, and *Dach* families in the mouse PT at ZT8 in the long-day condition was detected by RI in situ hybridization. Scale bar represent 300 μm.

(B) The *TSH*β promoter (−7.7 kbp, −0.6 kbp, −0.2 kbp, and −0.1 kbp) is activated by EYA3 and SIX1.

(C) Left: evolutionary conservation scores among vertebrate species were obtained from the UCSC Genome Browser (http://genome.ucsc.edu/). Genomic positions relative to the transcription start site (TSS, also designated as "−1") of the 0.6 kbp, 0.2 kbp, and 0.1 kbp *TSH*β promoter constructs are indicated. Right: the MEF3 site, D box, and So sites in the 0.1 kbp *TSH*β promoter are indicated. Colored letters indicate nucleotides matching the consensus sequence of the MEF3 site, D box, and So sites.

(D) The *TSH*β promoter (−0.1 kbp) is activated by EYA3 in a dose-dependent manner with or without SIX1 (Supplemental Experimental Procedures).

(E) The *TSH*β promoter (−0.1 kbp) and its MEF3-deleted [P(*TSH*β-ΔMEF3)], MEF3-mutated [P(*TSH*β-mutMEF3)], and D box-mutated [P(*TSH*β-mutD)] forms are activated by EYA3 and SIX1.

into two groups. One group was maintained under the short-day conditions and the other was housed under long-day conditions (light:dark = 16:8 hr, ZT0 = lights-on, ZT16 = lights-off, 400 lux) for 2 weeks. Mice in both groups were sacrificed and their PTs were sampled every 4 hr for 1 day, starting at ZT0.

For the acute long-day experiments, mice were first housed under short-day conditions for 3 weeks as described above and then separated into two groups. In one, the lights-on timing was advanced by 8 hr (advance condition), and in the other, the lights-off timing was delayed by 8 hr (delay condition). In both cases, photoperiod was extended by 8 hr. PTs from both groups were obtained every 4 hr for 1 day, starting at the lights-on time (ZT16 in the advance condition and ZT0 in the delay condition, when ZT was defined in the short-day condition).

This study was performed in compliance with the Rules and Regulations of the Animal Care and Use Committee, Kinki University School of Medicine, and carefully followed the Guide for the Care and Use of Laboratory Animals, Kinki University School of Medicine. Mice were also carefully kept and handled according to the RIKEN Regulations for Animal Experiments.

### Sampling of PT

Slices (0.5 mm thick) of the brain of CBA/N mice were cut on a mouse brain matrix (Neuroscience, Inc., Tokyo) and frozen, and the PT was punched out with a microdissecting needle (gauge 0.5 mm) under a stereomicroscope. The samples included a small amount of the surrounding tissue, such as the median eminence and ependymal cells. We sampled 25 mice at each time point. This entire procedure was repeated twice (n = 2) to obtain experimental replicates.

### Microarray Analysis

Total RNA was prepared from the pooled PT samples obtained at each time point under each condition using TRIzol reagent (GIBCO). cDNA synthesis and cRNA labeling reactions were performed as described previously [31]. Affymetrix high-density oligonucleotide arrays for *Mus musculus* (GeneChip Mouse Genome 430 2.0) were hybridized, stained, and washed according to the Expression Analysis Technical Manual (Affymetrix). The expression values were summarized by the robust multiarray analysis method [32]. The microarray data are available at the NCBI Gene Expression Omnibus (GSE24775) or at our website (http://photoperiodism.brainstars.org/).

### Accession Numbers

Microarray data reported herein have been deposited in the NCBI Gene Expression Omnibus with the accession number GSE24775.

### Supplemental Information

Supplemental Information includes Supplemental Results and Discussion, two figures, four tables, and Supplemental Experimental Procedures and can be found with this article online at doi:10.1016/j.cub.2010.11.038.

### Acknowledgments

We thank Joseph Takahashi for *mPer2*$^{Luc}$ mice and Yoichi Minami and Masayuki Iigo for helpful discussions. We also thank Junko Sakai and Yoko Sakakida for technical assistance. Some calculations were performed by the RIKEN Super Combined Cluster. This work was performed as a part of the Genome Network Project of the Ministry of Education, Culture, Sports, Science and Technology of Japan (H.R.U.). This research was supported by an intramural Grant-in-Aid from the RIKEN Center for Developmental Biology (H.R.U.), the RIKEN President's Fund (H.R.U.), and a Grant-in-Aid for Scientific Research (C) from the Ministry of Education, Culture, Sports, Science and Technology of Japan (Y.S.).

Received: October 17, 2010
Revised: November 10, 2010
Accepted: November 12, 2010
Published online: December 2, 2010

### References

1. Dawson, A., King, V.M., Bentley, G.E., and Ball, G.F. (2001). Photoperiodic control of seasonality in birds. J. Biol. Rhythms *16*, 365–380.
2. Ebling, F.J., and Barrett, P. (2008). The regulation of seasonal changes in food intake and body weight. J. Neuroendocrinol. *20*, 827–833.
3. Revel, F.G., Masson-Pévet, M., Pévet, P., Mikkelsen, J.D., and Simonneaux, V. (2009). Melatonin controls seasonal breeding by a network of hypothalamic targets. Neuroendocrinology *90*, 1–14.
4. Nakao, N., Ono, H., Yamamura, T., Anraku, T., Takagi, T., Higashi, K., Yasuo, S., Katou, Y., Kageyama, S., Uno, Y., et al. (2008). Thyrotrophin in the pars tuberalis triggers photoperiodic response. Nature *452*, 317–322.
5. Nakao, N., Ono, H., and Yoshimura, T. (2008). Thyroid hormones and seasonal reproductive neuroendocrine interactions. Reproduction *136*, 1–8.
6. Ono, H., Hoshino, Y., Yasuo, S., Watanabe, M., Nakane, Y., Murai, A., Ebihara, S., Korf, H.W., and Yoshimura, T. (2008). Involvement of thyrotropin in photoperiodic signal transduction in mice. Proc. Natl. Acad. Sci. USA *105*, 18238–18242.
7. Reiter, R.J. (1993). The melatonin rhythm: Both a clock and a calendar. Experientia *49*, 654–664.
8. Lincoln, G.A., Andersson, H., and Loudon, A. (2003). Clock genes in calendar cells as the basis of annual timekeeping in mammals—a unifying hypothesis. J. Endocrinol. *179*, 1–13.
9. Ikegami, K., Katou, Y., Higashi, K., and Yoshimura, T. (2009). Localization of circadian clock protein BMAL1 in the photoperiodic signal transduction machinery in Japanese quail. J. Comp. Neurol. *517*, 397–404.
10. Hoffman, R.A., and Reiter, R.J. (1965). Pineal gland: Influence on gonads of male hamsters. Science *148*, 1609–1611.
11. Bittman, E.L., Karsch, F.J., and Hopkins, J.W. (1983). Role of the pineal gland in ovine photoperiodism: Regulation of seasonal breeding and negative feedback effects of estradiol upon luteinizing hormone secretion. Endocrinology *113*, 329–336.
12. Morgan, P.J., and Williams, L.M. (1996). The pars tuberalis of the pituitary: A gateway for neuroendocrine output. Rev. Reprod. *1*, 153–161.
13. Goldman, B.D. (2001). Mammalian photoperiodic system: Formal properties and neuroendocrine mechanisms of photoperiodic time measurement. J. Biol. Rhythms *16*, 283–301.
14. Hazlerigg, D., and Loudon, A. (2008). New insights into ancient seasonal life timers. Curr. Biol. *18*, R795–R804.
15. Klosen, P., Bienvenu, C., Demarteau, O., Dardente, H., Guerrero, H., Pévet, P., and Masson-Pévet, M. (2002). The mt1 melatonin receptor and RORbeta receptor are co-localized in specific TSH-immunoreactive cells in the pars tuberalis of the rat pituitary. J. Histochem. Cytochem. *50*, 1647–1657.
16. Guilding, C., Hughes, A.T., Brown, T.M., Namvar, S., and Piggins, H.D. (2009). A riot of rhythms: Neuronal and glial circadian oscillators in the mediobasal hypothalamus. Mol. Brain *2*, 28.
17. Dupré, S.M., Miedzinska, K., Duval, C.V., Yu, L., Goodman, R.L., Lincoln, G.A., Davis, J.R., McNeilly, A.S., Burt, D.D., and Loudon, A.S. (2010). Identification of Eya3 and TAC1 as long-day signals in the sheep pituitary. Curr. Biol. *20*, 829–835.
18. Minami, Y., Kasukawa, T., Kakazu, Y., Iigo, M., Sugimoto, M., Ikeda, S., Yasui, A., van der Horst, G.T., Soga, T., and Ueda, H.R. (2009). Measurement of internal body time by blood metabolomics. Proc. Natl. Acad. Sci. USA *106*, 9890–9895.
19. Ueda, H.R., Chen, W., Minami, Y., Honma, S., Honma, K., Iino, M., and Hashimoto, S. (2004). Molecular-timetable methods for detection of body time and rhythm disorders from single-time-point genome-wide expression profiles. Proc. Natl. Acad. Sci. USA *101*, 11227–11232.
20. Jeong, B.C., Hong, C.Y., Chattopadhyay, S., Park, J.H., Gong, E.Y., Kim, H.J., Chun, S.Y., and Lee, K. (2004). Androgen receptor corepressor-19 kDa (ARR19), a leucine-rich protein that represses the transcriptional activity of androgen receptor through recruitment of histone deacetylase. Mol. Endocrinol. *18*, 13–25.

(F) The *TSH*β promoter (−0.1 kbp) and its So2-deleted form [P(*TSH*β-ΔSo2)] are activated by EYA3 and SIX, whereas its So1-deleted form [P(*TSH*β-ΔSo1)] is not.

In (B) and (D)–(F), each of the indicated promoters was fused to a luciferase reporter gene and used to transiently transfect NIH 3T3 cells. The luciferase activity for each promoter is expressed relative to activity with an empty vector. Data are representative of two independent experiments. Error bars represent ± SEM (n = 3).

21. Gordon, J.W., Pagiatakis, C., Salma, J., Du, M., Andreucci, J.J., Zhao, J., Hou, G., Perry, R.L., Dan, Q., Courtman, D., et al. (2009). Protein kinase A-regulated assembly of a MEF2·HDAC4 repressor complex controls c-Jun expression in vascular smooth muscle cells. J. Biol. Chem. *284*, 19027–19042.
22. Xu, P.X., Woo, I., Her, H., Beier, D.R., and Maas, R.L. (1997). Mouse Eya homologues of the Drosophila eyes absent gene require Pax6 for expression in lens and nasal placode. Development *124*, 219–231.
23. Borsani, G., DeGrandi, A., Ballabio, A., Bulfone, A., Bernard, L., Banfi, S., Gattuso, C., Mariani, M., Dixon, M., Donnai, D., et al. (1999). EYA4, a novel vertebrate gene related to Drosophila eyes absent. Hum. Mol. Genet. *8*, 11–23.
24. Bonini, N.M., Leiserson, W.M., and Benzer, S. (1993). The eyes absent gene: Genetic control of cell survival and differentiation in the developing Drosophila eye. Cell *72*, 379–395.
25. Bonini, N.M., Leiserson, W.M., and Benzer, S. (1998). Multiple roles of the eyes absent gene in Drosophila. Dev. Biol. *196*, 42–57.
26. Spitz, F., Demignon, J., Porteu, A., Kahn, A., Concordet, J.P., Daegelen, D., and Maire, P. (1998). Expression of myogenin during embryogenesis is controlled by Six/sine oculis homeoproteins through a conserved MEF3 binding site. Proc. Natl. Acad. Sci. USA *95*, 14220–14225.
27. Li, X., Oghi, K.A., Zhang, J., Krones, A., Bush, K.T., Glass, C.K., Nigam, S.K., Aggarwal, A.K., Maas, R., Rose, D.W., and Rosenfeld, M.G. (2003). Eya protein phosphatase activity regulates Six1-Dach-Eya transcriptional effects in mammalian organogenesis. Nature *426*, 247–254.
28. Pauli, T., Seimiya, M., Blanco, J., and Gehring, W.J. (2005). Identification of functional sine oculis motifs in the autoregulatory element of its own gene, in the eyeless enhancer and in the signalling gene hedgehog. Development *132*, 2771–2782.
29. Giordani, J., Bajard, L., Demignon, J., Daubas, P., Buckingham, M., and Maire, P. (2007). Six proteins regulate the activation of Myf5 expression in embryonic mouse limbs. Proc. Natl. Acad. Sci. USA *104*, 11310–11315.
30. Drolet, D.W., Scully, K.M., Simmons, D.M., Wegner, M., Chu, K.T., Swanson, L.W., and Rosenfeld, M.G. (1991). TEF, a transcription factor expressed specifically in the anterior pituitary during embryogenesis, defines a new class of leucine zipper proteins. Genes Dev. *5*, 1739–1753.
31. Ueda, H.R., Matsumoto, A., Kawamura, M., Iino, M., Tanimura, T., and Hashimoto, S. (2002). Genome-wide transcriptional orchestration of circadian rhythms in Drosophila. J. Biol. Chem. *277*, 14048–14052.
32. Irizarry, R.A., Bolstad, B.M., Collin, F., Cope, L.M., Hobbs, B., and Speed, T.P. (2003). Summaries of Affymetrix GeneChip probe level data. Nucleic Acids Res. *31*, e15.